Localized rotating-modes in capacitively coupled intrinsic Josephson junctions: Systematic study of branching structure and collective dynamical instability

M. Machida
CCSE, Japan Atomic Energy Research Institute, 6-9-3 Higashi-Ueno, Taito-ku, Tokyo 110-0015, Japan

T. Koyama
IMR, Tohoku University, 2-1-1 Katahira Aoba-ku, Sendai 980-8577, Japan
(Received 22 March 2004; published 30 July 2004)

A variety of the $I-V$ characteristics observed in a stack of intrinsic Josephson junctions is systematically explained in terms of the dynamics of the localized rotating mode in the discrete nonlinear systems. We clarify the effect of the capacitive coupling constant on the $I-V$ characteristics, using the capacitively coupled Josephson junction model. The branch structure in the $I-V$ characteristics changes from an assembly of equidistance branches to a single hysteresis-loop-like structure as the capacitive coupling constant increases. This behavior is in accordance with experiments. We predict that dynamical transitions between collective rotating states take place in the resistive state of a stack of intrinsic Josephson junctions in the strong capacitive coupling regime. These transitions create step-like structure in the $I-V$ characteristics, which is observed in $La_{1-x}Sr_xCuO_{4-\delta}$.

DOI: 10.1103/PhysRevB.70.024523 PACS number(s): 74.81.Fa, 74.50.+r, 63.20.Pw

I. INTRODUCTION

Layered high-T_c superconductors can be considered as naturally stacked Josephson junctions (intrinsic Josephson junctions).[1] The dynamics of the superconducting phase differences in the intrinsic Josephson junctions have attracted a great interest. It is well known that the phase differences in the intrinsic Josephson junctions are affected by the inductive coupling between junctions in the presence of a magnetic field and also by the charge-imbalance effect[2] and the phonon effect.[3] Furthermore, since the superconducting layers forming the junctions are extremely thin in the intrinsic Josephson junctions, a type of capacitive coupling appears between the junctions, which originates from the breakdown of the charge neutrality in thin superconducting layers as discussed in Refs. 4 and 5. The capacitive coupling dominates the phase dynamics of the intrinsic Josephson junctions when no external magnetic field is applied and the charge imbalancing effect can be neglected. A new model which describes the phase dynamics of an array of capacitvely coupled Josephson junctions (CCJJ) was proposed in Refs. 4 and 5. The c-axis $I-V$ characteristics of Bi-2212 under no external magnetic field has been successfully analyzed on the basis of this model.[4–6]

In this paper, we present a systematic study for the dynamics of the CCJJ model, focusing on the dependence of the phase dynamics on the strength of the capacitive coupling constant from weak to strong coupling regimes. The charge imbalance effect is not considered in this paper. As discussed in Ref. 6, this effect may be incorporated phenomenologically into our model by including a Drude-like damping term in the capacitive coupling constant, which describes the relaxation of total charge. The effect is important for a *quantitative* analysis of the $I-V$ charactristics of a stack of intrinsic Josephson junctions, but it cannot explain the large difference in the $I-V$ characteristics between $Bi_2Sr_2CaCu_2O_8$ (Bi-2212) with a weak capacitive coupling constant and $La_{1-x}Sr_xCuO_{4-\delta}$ (LSCO) with a strong one. Then, the effect is ignored in the present paper for theoretical clearness.[7]

It is known that the CCJJ model shows two types of dynamics[5,6,8] i.e., the plane-wave like propagating mode called the longitudinal Josephson plasma[4,5] and the localized rotating-mode peculiar to the discrete nonlinear systems.[9] Both modes have been detected in high-T_c superconductors, namely the longitudinal Josephson plasma has been found in the microwave absorption experiments in Bi-2212[10] and the latter localized mode has been identified to be the origin of the multiple-branch structure in the $I-V$ characteristics of Bi-2212.[5,11] From this fact a stack of intrinsic Josephson junctions is understood to be the realistic discrete nonlinear system having the intrinsic localized excitation modes. Hence, using the CCJJ model, one can study the dynamics of both linear propagating mode and the nonlinear localized one in detail, which is currently under intensive studies in nonlinear physics.[12]

There are two mechanisms which cause the localization in dynamical systems. As is well known, phonons, conduction electrons, etc. in low dimensional systems are localized by the effect of randomly distributed disorders. The localization of this kind originates from the lack of translational invariance. There is another type of localization phenomena being independent of disorders, which stems from the lattice discreteness and the nonlinear interaction in a dynamidal system.[12] The localized mode of this kind is called the nonlinear localized mode or the discrete breathers.[12] It has been reported that these localized modes have been detected in lattice-vibration modes[13] and spin-wave excitations[14] in some crystal lattices and also in the phase-oscillation modes in conventional Josephson junctions.[15] However, these excitations are rather special, and the experimental confirmations are not easily accessible in these systems.

Recently, it has been recognized that the capacitive coupling constant takes various values covering the weak to

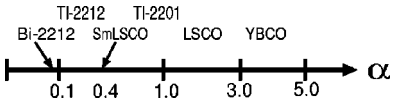

FIG. 1. Estimated values of the capacitive coupling constant α in high-T_c superconductors: $Bi_2Sr_2CaCu_2O_8$ (Bi-2212) (Refs. 5 and 8), $Tl_2Ba_2CaCu_2O_8$ (Tl-2212) (Ref. 16), $Tl_2Ba_2CuO_6$ (Tl-2201) (Ref. 16), $SmLa_{1-x}Sr_xCuO_{4-\delta}$ (SmLSCO) (Ref. 17), $La_{1-x}Sr_xCuO_{4-\delta}$ (LSCO) (Ref. 18), and $YBa_2CaCu_3O_{7-\delta}$ ($\delta=0.3 \sim 0.5$) (YBCO) (Ref. 19). These values are roughly evaluated by using material parameters (dielectric constant and lattice constant) and (or) by the analysis of the $I-V$ characteristics.

strong coupling regimes in high-T_c superconductors and also in layered organic superconductors, that is, the capacitive coupling is tunable in these systems. This fact indicates that the systematic studies on the nonlinear localized modes are possible under various values of the nonlinear coupling constant in a stack of intrinsic Josephson junctions. Figure 1 shows roughly estimated values of the capacitive coupling constant α defined as $\alpha=\epsilon\mu^2/sD$ in several high-T_c superconductors, where ϵ, μ, s, and D are the dielectric constant of the block layers, the charge screening length of the superconducting layers, the thickness of the superconducting, and the insulating layers, respectively.[4] For example, we find $\alpha \simeq 0.1$ in $Bi_2Sr_2CaCu_2O_8$ (Bi-2212), $\alpha \simeq 0.4$ in $SmLa_{1-x}Sr_xCuO_{4-\delta}$,[17] and $\alpha \simeq 1.0-3.0$ in $La_{1-x}Sr_xCuO_{4-\delta}$ (LSCO). These values were evaluated by the analysis of the experimental data for the c-axis transport or optical properties. From these results one understands that Bi-2212 is in the weak-coupling regime ($\alpha \ll 1.0$), whereas LSCO is in the relatively strong-coupling regime ($\alpha > 1$). The $I-V$ characteristics in the weak coupling regimes are very different from that in the strong one, that is, they depends strongly on α. Here, we briefly summarize the difference in the $I-V$ characteristics between Bi-2212 and LSCO. In Bi-2212 the multiple branch structure is commonly seen in the $I-V$ characteristics.[20] The number of branches is understood to be nearly equal to the number of junctions. On the other hand, the multiple branch structure is not seen in LSCO and a single or a few hysteresis loops constitute the $I-V$ characteristics.[18] The step-like structure with an almost equal spacing, which is not seen in Bi-2212, is also observed on the resistive branch in LSCO, indicating some dynamical instabilities taking place at the steps.[18]

In this paper we present a systematic study on the nonlinear localized modes covering both strong and weak coupling regimes, using the CCJJ model. The $I-V$ characteristics is investigated as a function of the capacitive coupling constant α. We clarify the change in the dynamics of the localized rotating modes as the coupling constant increases. It is also shown that a series of dynamical transitions, as observed in LSCO, takes place in the strong coupling regime. At the transition points the collective motion of the localized rotating modes changes.

II. MODEL AND NUMERICAL SIMULATION

In the CCJJ model the dynamics of the gauge-invariant phase difference $P_{\ell+1,\ell}(t)$ ($\equiv \theta_{\ell+1}-\theta_\ell-\phi_0/2\pi\int_\ell^{\ell+1} A_z dz$) between ℓth and $(\ell+1)$-th superconducting layers is described by the equation:

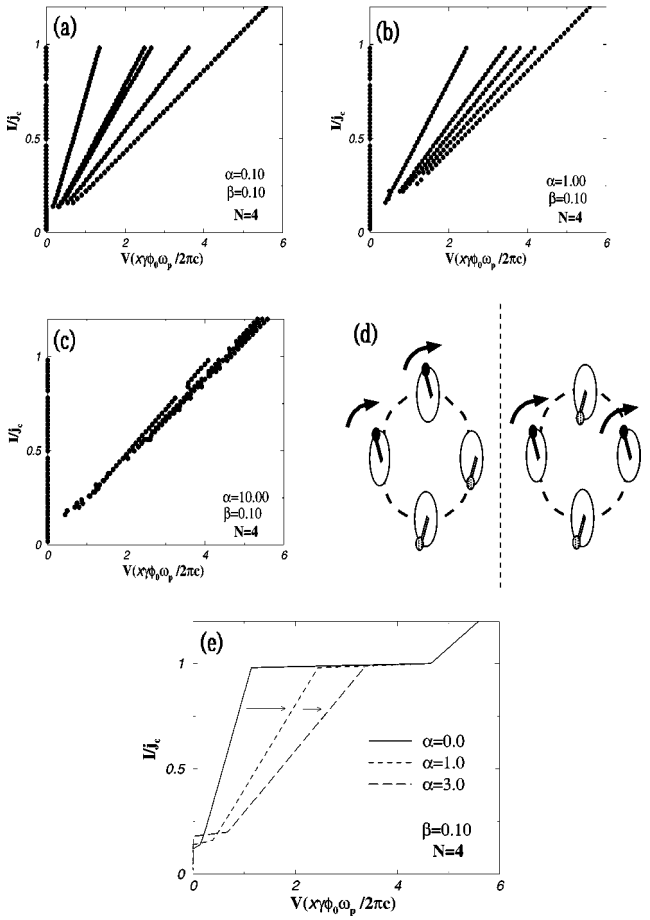

FIG. 2. The branch structure in the $I-V$ characteristics in four-junction systems: (a) $\alpha=0.10$, (b) $\alpha=1.00$, and (c) $\alpha=10.0$ The periodic boundary condition is imposed. (d) Schematic view for the two nonequivalent configurations in the periodic boundary condition in which two localized rotating modes are excited; (e) the α dependence of the first branch.

$$\frac{1}{\omega_p^2}\partial_t^2 P_{\ell+1,\ell}(t) + \frac{\beta}{\omega_p}\partial_t P_{\ell+1,\ell}(t) + \sin P_{\ell+1,\ell}(t) = \alpha[\sin P_{\ell+2,\ell+1}(t) - 2\sin P_{\ell+1,\ell}(t) + \sin P_{\ell,\ell-1}(t)] + I/j_c, \tag{1}$$

where ω_p, j_c, and I are, respectively, the plasma frequency, the Josephson critical current, and the external dc current, and β is related with the McCumber parameter β_c as $\beta = 1/\sqrt{\beta_c}$.[5] Note that the CCJJ model is different from the conventional RCSJ (resistively and capacitively shunted junction) model only by the term including α which gives the coupling between junctions stemming from the charging effect. We also notice that the dynamical system described by Eq. (1) is equivalent to an array of nonlinearly coupled pendulums. In deriving Eq. (1) we assume the relation between the charge density ρ_ℓ in ℓth superconducting layer and the scalar potential φ_ℓ as

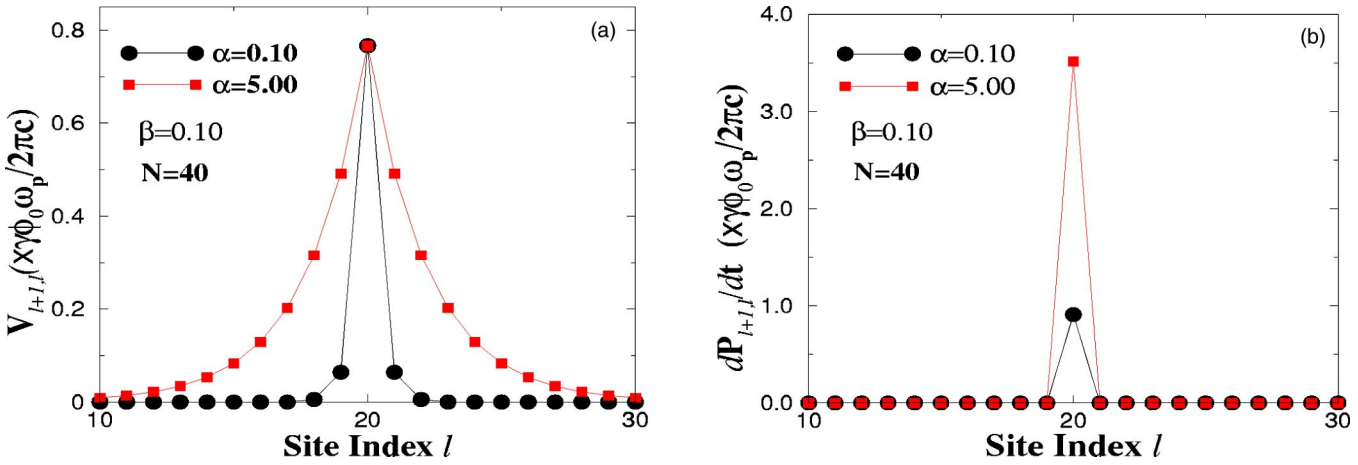

FIG. 3. (Color online) (a) Voltage distribution (Ref. 21) in the first branch for $\alpha=0.10$ and $\alpha=5.00$. The periodic boundary condition is imposed on the system with $N=40$; (b) distribution of $dP_{\ell+1,\ell}/(dt)$.

$$\rho_\ell = -\frac{1}{4\pi\lambda_e^2}\left(\varphi_\ell + \frac{\phi_0}{2\pi c}\frac{\partial\theta_\ell}{\partial t}\right). \tag{2}$$

$$\frac{\phi_0}{2\pi c}\frac{\partial P_{\ell+1,\ell}}{\partial t} = \alpha[-V_{\ell,\ell-1} + (2+1/\alpha)V_{\ell+1,\ell} - V_{\ell+2,\ell+1}]. \tag{3}$$

The charge ρ_ℓ given in Eq. (2), which induces the capacitive coupling between junctions, cannot be neglected in the present intrinsic Josephson junctions, though it is negligibly small in conventional systems. In the presence of ρ_ℓ the Josephson relation between voltage $V_{\ell+1,\ell}$ and time derivative of the phase difference (rotating velocity) $\partial P_{\ell+1,\ell}/\partial t$ is generalized as[4,5]

Thus, the voltage in a junction site depends not only on the on-site rotating velocity but also on those in the neighboring junctions. In this paper we solve Eq. (1) in the range of $0.0<\alpha<10.0$ and examine how the dynamics of the phase differences changes with varying the value of α.

The numerical procedure is summarized as follows. First, we solve Eq. (1) for various fixed values of I and obtain the

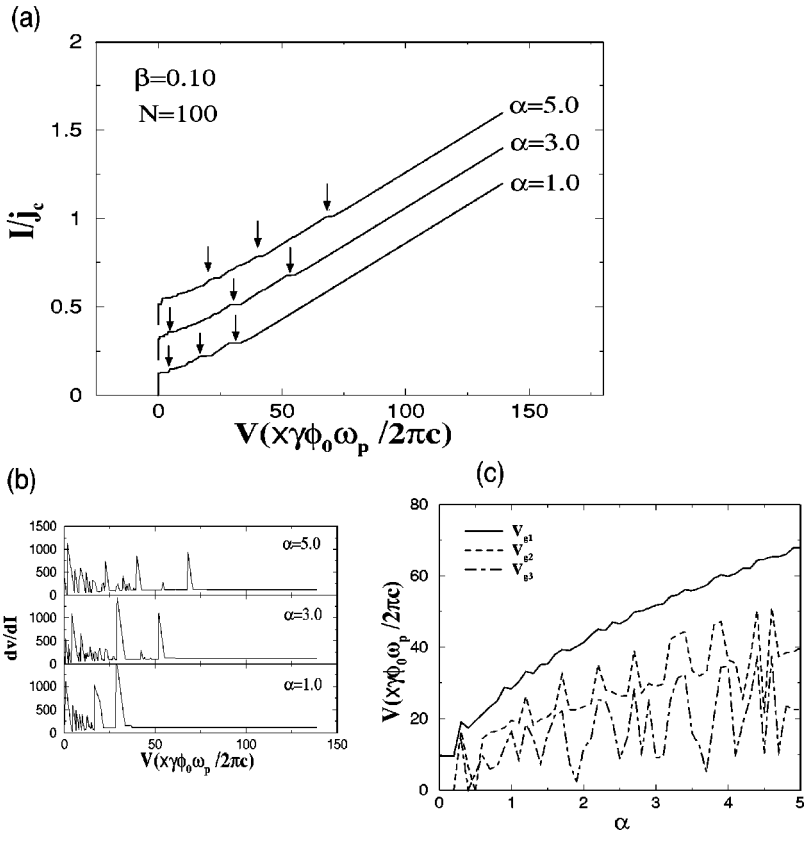

FIG. 4. (a) $I-V$ characteristics for three different values of α. The $I-V$ curves for $\alpha=3.0$ and 5.0 are moved upward for avoiding the overlap. Step-like structure appears at the positions indicated by arrows; (b) the voltage dependence of dV/dI. A few high peaks are clearly distinguishable, and their voltage positions are assigned as V_{g1}, V_{g2}, and V_{g3} from the low voltage side; (c) the α dependence of V_{g1}, V_{g2}, and V_{g3}.

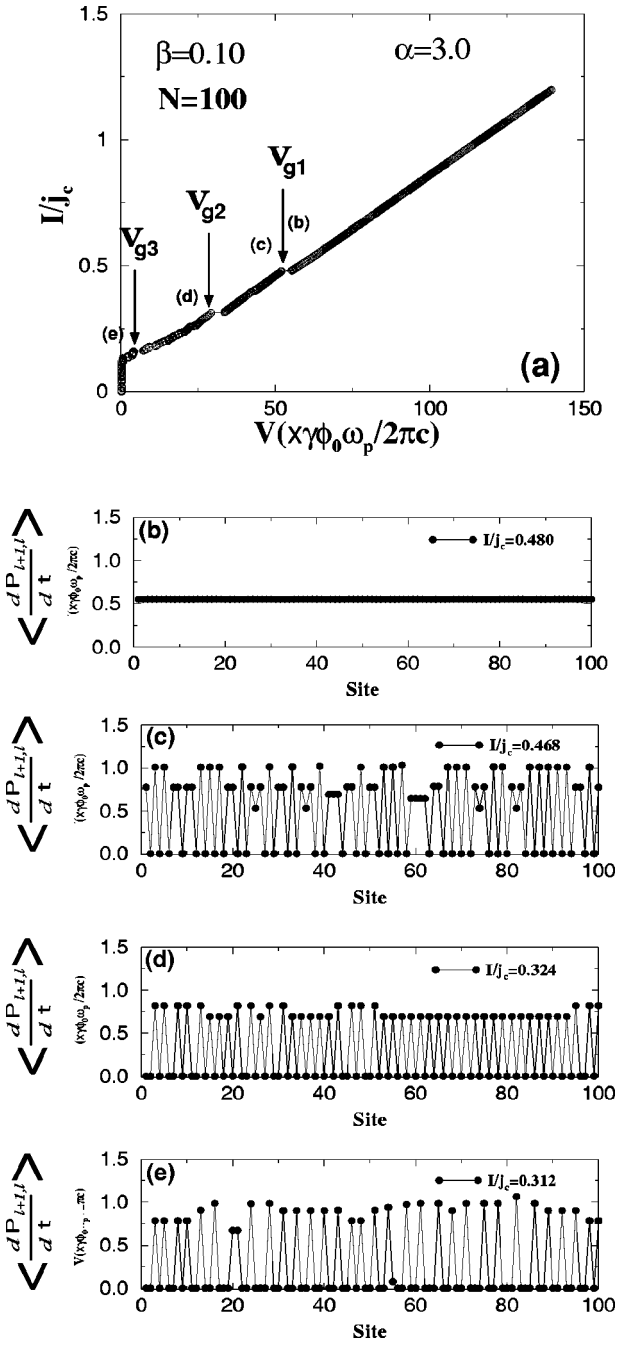

FIG. 5. (a) $I-V$ characteristics for $\alpha=3.0$. The site distributions of $\langle dP_{\ell+1,\ell}/dt\rangle$, (b) above, and (c) below V_{g1}, (d) below V_{g2}, and (e) below V_{g3}.

time-dependent phase differences, using the fourth-order Runge–Kutta algorithm. To avoid the boundary effect which breaks the translational symmetry of the system, we adopt the periodic boundary condition in the present calculations. The voltage appearing in each junction, $V_{\ell+1,\ell}$, is obtained using the generalized Josephson relation given in Eq. (3), from which one can acquire the current-biased $I-V$ characteristics. In the numerical simulations we search all kinds of stable rotating motion in this system under a fixed current value I by running parallel simulations over more than 100 CPU for randomly selected initial conditions. After sufficient long time, the system reaches a certain steady state depending on the initial condition. For example, in the case of $I=0.5j_c$ in a four-junction system the time-averaged total voltage converges on one of six values, depending on the initial conditions in the weak coupling case, i.e., $\alpha=0.1$, as seen in Fig. 2(a). When the time-averaged total voltages in the steady states are plotted as a function of the bias current, one obtains the $I-V$ characteristics, as seen in Figs. 2(a)–2(c). In the weak coupling regime ($\alpha<1$), the multiple branch structure with nearly equal spacing appears in the $I-V$ characteristics. In this case we have five resistive branches, though the number of junctions is 4 in this system. The branches are numbered from 1 to 5 in ascending order of voltages. In the first branch the localized rotating mode appears on one of the four junctions, while it appears on two sites in the second and the third branches. As seen in Fig. 2(d), there are two nonequivalent configurations in the case where the number of rotating sites is two in the periodic boundary condition, i.e., the confugurations in which alternate junctions or two consecutive junctions are resistive. These two configurations are not degenerate in the presence of the capacitive coupling and then their $I-V$ curves weakly separate out and form a pair. Such pairs of the $I-V$ curves have been frequently observed in the intrinsic Josephson junctions (Bi-2212).[22]

Let us next investigate the case with a larger value of α. As seen in Fig. 2(b), the resistive branches from 1 to 4 shift towards the higher voltage side as α is increased. Furthermore, in the case of $\alpha=10.0$ all the branches reach the outermost one as seen in Fig. 2(c). In this region all the junctions are in the rotating state, that is, the localized rotating state is not stable in the strong coupling region. The $I-V$ characteristics similar to that given in Figs. 2(b) and 2(c) have been observed in the intrinsic Josephson junction systems, as well.[18] Let us now focus on the voltage shift in the first branch with increase of the value of α. Figure 2(e) shows the shifts for three different values of α. As seen in this figure, the first hysteresis loop expands as the capacitive coupling increases. This effect is understood in the following way. When α becomes larger, the number of charging superconducting layers near the rotating junction site is increased (see below), that is, the charging energy in the system increases with increasing the value of the capacitive coupling constant. Then, the resistive branch shifts towards the higher voltage side.

Let us next examine the α dependence of the isolated localized rotating modes in more detail.[8] Figure 3(a) shows the spatial variation of the local voltage[21] in the system composed of 40 junctions in the weak ($\alpha=0.1$) and strong ($\alpha=5.0$) coupling regions under a fixed bias current. In Fig. 3(b), we also plot the rotation velocity in this case, i.e., the time average of $dP_{\ell+1,\ell}/(dt)$. From these figures one can see that the rotating motion is confined within a single junction site in both cases, but the voltage is not confined in the rotating junction site but is widely distributed over many junctions especially in the strong coupling case. This result indicates that the voltage required to excite a localized rotating mode increases as the capacitive coupling becomes larger [see Fig. 2(e)].[8] Consequently, the switching probabilty from an oscillating state to a localized rotating one is suppressed in the strong coupling region. The multiple branch structure

is, thus, hardly realized in the strong coupling region. This result explains why the multiple branch structure is not observed in LSCO with a larger value of α.[18]

Next, we study the collective rotating states in which several junctions are in the rotating state. We concentrate on the outermost resistive branch in the CCJJ model. Uematsu *et al.* found regular step-like structures in the $I-V$ characteristics in LSCO.[18] They claim that this structure originates from the resonance with the longitudinal Josephson plasma.[18] To clarify the origin we perform more elaborate simulations in a system of 100 junctions under the periodic boundary condition. In these simulations, the current is decreased from $1.2j_c$ to $0.0j_c$ to simulate the experimental situations. Figure 4(a) shows the $I-V$ curves for three different values of α, i.e., $\alpha=1.0$, 3.0, and 5.0. The step-like structure appears at the positions indicated by arrows on these curves. To make the positions of the steps clear we also plot dV/dI in these three cases in Fig. 4(b). We select three large peaks having peak values bigger than 500 in each case in Fig. 4(b) and denote the voltage values giving these peaks by V_{g1}, V_{g2}, and V_{g3} in order of decreasing voltage. The α dependence of these voltages is presented in Fig. 4(c). Although V_{g2} and V_{g3} show large fluctuations, these voltages are basically increasing functions of α and then the separations between the peak voltages increase as α becomes larger. In order that these steps are distinguishable in the $I-V$ curves these voltage values must be well separated with each other, that is, α should be large enough. This result is consistent with the experimental fact that the step-like structure is clearly seen in LSCO, but is not in Bi-2212, since α is large in LSCO but is very small in Bi-2212.

Now, let us study what occurs at the steps in the $I-V$ characteristics. We focus on a typical case of $\alpha=3.0$ below. Figure 5(a) shows the $I-V$ characteristics in the case of $\alpha=3.0$, in which the three steps are clearly seen. The spatial distributions of the time-averaged velocities $\langle dP_{\ell+1,\ell}/dt\rangle$ above and below the first step V_{g1} are presented in Figs. 5(b) and 5(c). Below V_{g1} about a half of the junctions changes to the nonrotating state. The average values $\langle dP_{\ell+1,\ell}/dt\rangle$ on the junction sites being in the rotating state are sorted into approximately four values and show the glassy-like disribution. We call this state the rotating rotor glass in which some localized modes are closely overlapped and the others are separated irregularly. The pattern of $\langle dP_{\ell+1,\ell}/dt\rangle$ is stable until the current is decreased to the value giving the next step at V_{g2}. Furthermore, we notice that the averages $\langle dP_{\ell+1,\ell}/dt\rangle$ in the rotating sites seen in Fig. 5(c) are larger than the value in the homogeneous rotating state in Fig. 5(b). This is because the voltage appearing at the rotating sites compensates the decrease at the nonrotating sites to keep the total voltage nearly the same, which implies that the localization of energy rapidly occurs at the instability point without a large mount of energy relaxation. At V_{g2} (V_{g3}) the velocity pattern changes from (c) to (d) [from (d) to (e)]. At these steps the number of rotating sites is found to be decreased. This result indicates that some of the rotating sites instantaneously absorb the energy of the other rotating sites at these steps. The transitions between the rotating rotor glasses will be seen in other measurements. For example, the spectrum of the Josephson emission is expected to change when one goes through the steps.

III. SUMMARY

In summary, we performed numerical simulations for the CCJJ model to clarify the origin of the variety observed in the $I-V$ characteristics of high-T_c cuprates. We studied the behavior of the localized rotating modes for various values of the coupling constant α and proved that the dynamics of these localized modes primarily determines the $I-V$ characteristics. Since the energy required to excite the localized rotating modes increases as the capacitive coupling increases, several junctions collectively rotate. As a result, the equidistant multiple-branch structure disappears in the strong coupling systems. This result explains why the multiple branch structure is not observed in LSCO. We also found that the transitions between the dynamical states occur in the current-decreasing process in the strong coupling regime. At these transitions the spatial pattern of the rotating motion changes and the system goes into the glassy phases. These transitions create step-like structure in the $I-V$ curves, which has been observed in LSCO. We emphasize that a stack of intrinsic Josephson junctions is the best system in which systematic studies on the localized rotating modes are possible.

ACKNOWLEDGMENTS

One of the authors (M.M.) thanks A. E. Koshelev, T. Yamashita, S. Uematsu, S. Takeno, M. Tachiki, C. H. Helm, and N. Sasa for illuminating discussions, both authors thank CREST (JST) for financial support.

[1] R. Kleiner, F. Steinmeyer, G. Kunkel, and P. Müller, Phys. Rev. Lett. **68**, 2394 (1992); G. Oya, N. Aoyama, A. Irie, S. Kishida, and H. Tokutaka, Jpn. J. Appl. Phys., Part 2 **31**, L829 (1992).

[2] D. A. Ryndyk, Phys. Rev. Lett. **80**, 3376 (1998); D. A. Ryndyk, J. Keller, and C. Helm, J. Phys.: Condens. Matter **14**, 815 (2002).

[3] Ch. Helm, Ch. Preis, F. Forsthofer, J. Keller, K. Schlenga, R. Kleiner, and P. Müller, Phys. Rev. Lett. **79**, 737 (1997); Ch. Preis, Ch. Helm, K. Schmalzl, J. Keller, R. Kleiner, and P. Müller, Physica C **362**, 51 (2001).

[4] T. Koyama and M. Tachiki, Phys. Rev. B **54**, 16 183 (1996).

[5] M. Machida, T. Koyama, and M. Tachiki, Phys. Rev. Lett. **83**, 4618 (1999).

[6] H. Matsumoto, S. Sakamoto, F. Wajima, T. Koyama, and M. Machida, Phys. Rev. B **60**, 3666 (1999).

[7] Note that the charge imbalance effect takes place in the superconducting layers, that is, the effect primarily depends on the nature of the superconducting layers, not the interlayer coupling. Thus,

the strength of the charge imbalance effect is expected to be much the same in both Bi-2212 and LSCO which show qualitatively different $I-V$ characteristics.

[8] Ch. Preis, Ch. Helm, J. Keller, A. Sergeev, and R. Kleiner, SPIE Conference Proceedings "Superconducting Superlattices II" (1998), p. 236.

[9] S. Takeno and M. Peyard, Physica D **92**, 140 (1996).

[10] I. Kakeya, K. Kindo, K. Kadowaki, S. Takahashi, and T. Mochiku, Phys. Rev. B **57**, 3108 (1998); M. B. Gaifullin, Y. Matsuda, N. Chikumoto, J. Shimoyama, K. Kishio, and R. Yoshizaki, Phys. Rev. Lett. **83**, 3928 (1999).

[11] S. Takeno, J. Phys. Soc. Jpn. **69**, 213 (2000).

[12] A. J. Sievers and S. Takeno, Phys. Rev. Lett. **61**, 970 (1988); for a review, see S. Flach and C. R. Willis, Phys. Rep. **295**, 181 (1998).

[13] B. I. Swanson, J. A. Brozik, S. P. Love, G. F. Strouse, A. P. Shreve, A. R. Bishop, W. Z. Wang, and M. I. Salkola, Phys. Rev. Lett. **82**, 3288 (1999).

[14] U. T. Schwarz, L. Q. English, and A. J. Sievers, Phys. Rev. Lett. **83**, 223 (1999).

[15] E. Trias, J. J. Mazo, and T. P. Orlando, Phys. Rev. Lett. **84**, 741 (2000); P. Binder, D. Abraimov, A. V. Ustinov, S. Flach, and Y. Zolotaryuk, *ibid.* **84**, 745 (2000).

[16] We can roughly estimate values of α from the crystalline structure and the dielectric constant. See, e.g., A. A. Tsvetkov, D. van der Marel, K. A. Moler, J. R. Kirtley, J. L. de Boer, A. Meetsma, Z. F. Ren, N. Koleshnikov, D. Dulić, A. Damascelli, M. Grüninger, J. Schützmann, J. W. van der Eb, H. S. Somal, and J. H. Wang, Nature (London) **395**, 360 (1998); D. Dulić, D. van der Marel, A. A. Tsvetkov, W. N. Hardy, Z. F. Ren, J. H. Wang, and B. A. Willemsen, Phys. Rev. B **60**, R15 051 (1999).

[17] Ch. Helm, L. N. Bulaevskii, E. M. Chudnovsky, and M. P. Maley, Phys. Rev. Lett. **89**, 057003 (2002).

[18] Y. Uematsu, N. Sasaki, Y. Mizugaki, K. Nakajima, T. Yamashita, S. Watauchi, and I. Tanaka, Physica C **362**, 290 (2001).

[19] M. Rapp, A. Murk, R. Semerad, and W. Prusseit, Phys. Rev. Lett. **77**, 928 (1996).

[20] K. Schlenga, R. Kleiner, G. Hechtfischer, M. Mößle, S. Schmitt, P. Müller, Ch. Helm, Ch. Preis, F. Forsthofer, J. Keller, H. L. Johnson, M. Veith, and E. Steinbeiß, Phys. Rev. B **57**, 14 518 (1998), and references therein.

[21] The definition of the local voltage used in this paper is an integration of the electric field between neighboring superconducting layers. The chemical potential difference is dropped for simplicity.

[22] T. Yamashita (private communication).